FORWARD X-RAY AND ULTRAVIOLET SMITH-PURCELL RADIATION FOR FEL

A.A. Tishchenko*, D.Yu. Sergeeva, NRNU "MEPhI", Moscow, Russia

Abstract

Smith-Purcell radiation in X-Ray and UV frequency range is investigated. The particle is supposed to move at arbitrary angle to the rulings direction parallel to a grating surface. The radiation going both through the upper and forward target edges is taken into account. Spectral and angular characteristics of the forward radiation are discussed. The influence of oblique incidence of the particle to the grating in on the intensity of radiation is analyzed.

INTRODUCTION

The scheme of Free Electron Lasers based on Smith-Purcell effect is well known to describe the process of interaction between an electron beam and evanescent wave, which bunches this beam. In this work we concentrate on the process of generation of the radiation propagating at small angles. In terms of approach described in detail in [1]-[3], we investigate the Smith-Purcell radiation at oblique incidence of a single charged particle for X-Ray and UV frequency region. This forward radiation propagates through all region of the beam moving, whereas the usual surface waves existing in FELs [4] decrease exponentially with distance from the surface. Therefore, the forward radiation considered in this article is able to provide more close interaction between the beam and the radiation, than the surface waves.

FIELD OF RADIATION

Let the charge e moves with constant velocity $\mathbf{v}=(v_x, v_y, 0)$ at a distance h above the upper edge of a target. The target consists of N strips with dielectric permittivity $\varepsilon(\omega)$ with air between strips. The period of the grating is d. The size of a strip is (a,∞,b) (see Fig. 1). We find the radiation field using the polarization current method. The essence of this method is following. The Coulomb field of a moving particle $\mathbf{E}_0(\mathbf{r},\omega)$ acts upon material of the target and excites dynamically changed polarization currents in it. This leads to arising of the radiation determined by Fourier-image of the current density $\mathbf{j}(\mathbf{r},\omega)$:

$$\mathbf{j}(\mathbf{r},\omega)=\frac{\omega}{4\pi i}\left(\varepsilon(\omega)-1\right)\mathbf{E}_0(\mathbf{r},\omega). \tag{1}$$

For X-Ray frequency region

$$\omega \gg \omega_p \tag{2}$$

the dielectric function of a medium can be written as:

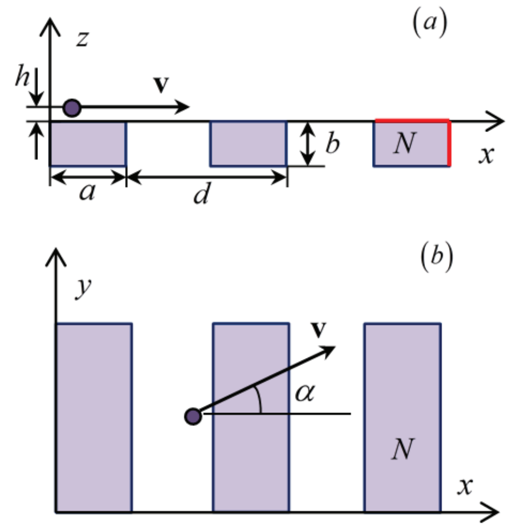

Figure 1: The geometry (a) side view, (b) top view.

$$\varepsilon = 1+\chi'+i\chi'', \tag{3}$$

where $\chi' = -\omega_p^2/\omega^2$, ω_p is the plasma frequency, which is usually in the range of 15 - 35 eV, in dependence on the target material. The case of absorbing medium can be of interest, for example, to deal with X-ray Cherenkov radiation [5], [6]; now we restrict our consideration to non-absorbing mediums only, i.e. $\chi'' \ll |\chi'|$. However, as the absorption in X-ray region plays a role mainly near narrow lines, our results remain valid in rather wide range of parameters.

The radiation field is determined by current density as

$$\mathbf{E}(\mathbf{r},\omega)=\frac{i\omega}{c^2}\frac{e^{ik'r}}{r}\left[\mathbf{n}\left[\mathbf{n}\int_V d^3r' e^{-i\mathbf{k}'\mathbf{r}'}\mathbf{j}(\mathbf{r}',\omega)\right]\right], \tag{4}$$

where it is integrated over the region of existence of polarization currents, i.e. over the target volume V; the prime in the designation of wave vector $\mathbf{k}'=\mathbf{n}'\sqrt{\varepsilon(\omega)}\,\omega/c$ stands for the value inside the matter.

To obtain the field of forward radiation we should take into account the refraction of radiation at two target edges: the upper one and the forward one (see the red lines in Fig. 1). Allowing for the law of refraction is important here because of periodicity of the target. The matter is that, despite the weakness of the effect of the refraction in X-ray range, for numerous periodic sources of radiation the effect of refraction is accumulated and becomes prominent.

*tishchenko@mephi.ru

ISBN 978-3-95450-133-5

In brief, we divide the effective area of integration V into two parts V_1 and V_2 in z-direction by plane $z = n'_z\left(x - a - sd\right)/n'_x$. Here s is the number of the strip. So, the radiation generated in the volume V_1 refracts at the upper edge, the radiation generated in the volume V_2 refracts at the forward edge.

The refraction laws for upper and forward edges give us the relations for the unit wave-vectors $\mathbf{n}_1$ and $\mathbf{n}_2$ of radiation propagating in V_1 and V_2 - inside the target, and $\mathbf{n}$ - out of the target:

$$\begin{aligned} \mathbf{n}_1 &= \varepsilon(\omega)^{-1/2}\left(n_x, n_y, \sqrt{\varepsilon(\omega) - 1 + n_z^2}\right), \\ \mathbf{n}_2 &= \varepsilon(\omega)^{-1/2}\left(\sqrt{\varepsilon(\omega) - 1 + n_x^2}, n_y, n_z\right). \end{aligned} \tag{5}$$

Generally speaking, there are two different situations when the laws of refraction are allowed for:

I. without taking into account inhomogeneous plane waves;

II. taking into account only inhomogeneous plane waves.

The case I is realized if $n_z^2 > 1 - \varepsilon(\omega)$; then z-component of the wave-vector in medium n_{1z} is real, which corresponds to the ordinary plane waves. The case II takes place if $n_z^2 < 1 - \varepsilon(\omega)$; then z-component of the wave-vector in medium n_{1z} is imaginary and it corresponds to the inhomogeneous evanescent waves.

The same situation can arise with the x-component of wave-vector, but it will give radiation mainly at the big angles. Our goal in this work is to analyse forward radiation, which accompanies and acts upon the moving beam during a considerable part of its way. So, below the condition $n_x^2 \geq 1 - \varepsilon(\omega)$ is thought to be always satisfied.

Let us start with the **first** more general **case** of $n_z^2 > 1 - \varepsilon(\omega)$. After integrating in Eq. (4) the total field of radiation takes the form:

$$\begin{aligned} \mathbf{E}(\mathbf{r},\omega) = &-i\frac{e(\varepsilon-1)}{4\pi v_x}\frac{1}{\rho}\frac{\omega^2}{c^2}\frac{e^{ikr}}{r}e^{-h\rho} \times \\ &\times\left\{\frac{\left[\mathbf{n}_1\left[\mathbf{n}_1\mathbf{L}\right]\right]}{t_1}\left(\frac{e^{i\varphi_1 a}-1}{i\varphi_1} - \frac{e^{i\varphi_1 a} - e^{-\frac{n_{1z}}{n_{1x}}t_1 a}}{i\varphi_1 + \frac{n_{1z}}{n_{1x}}t_1}\right)\sum_{s=1}^{N} e^{i\varphi_1(s-1)d} - \right. \\ &\left. -\frac{\left[\mathbf{n}_2\left[\mathbf{n}_2\mathbf{L}\right]\right]}{t_2}\left(\frac{e^{i\varphi_2 a}-1}{i\varphi_2}e^{-bt_2} - \frac{e^{i\varphi_2 a} - e^{-\frac{n_{2z}}{n_{2x}}t_2 a}}{i\varphi_2 + \frac{n_{2z}}{n_{2x}}t_2}\right)\sum_{s=1}^{N} e^{i\varphi_2(s-1)d}\right\}, \end{aligned} \tag{6}$$

where

$$\begin{aligned} &\mathbf{L} = \mathbf{A} - i\rho\mathbf{e}_z, \quad \mathbf{k} = \omega/c\,\mathbf{n}, t_{(1,2)} = \rho - i\sqrt{\varepsilon}k_{(1,2)z}, \\ &\mathbf{A} = \frac{\omega}{c\beta_x}\left\{1 - n_y\beta_y - \beta_x^2;\ \beta_x\left(n_y - \beta_y\right);\ 0\right\}, \\ &\rho = \frac{\omega}{c\beta_x}\sqrt{\left(1 - n_y\beta_y\right)^2 + n_y^2\beta_x^2 - \beta_x^2}, \\ &\varphi_1 = \frac{\omega}{c\beta_x}\left(1 - n_y\beta_y - n_x\beta_x\right), \\ &\varphi_2 = \frac{\omega}{c\beta_x}\left(1 - n_y\beta_y - \beta_x\sqrt{\varepsilon(\omega) - 1 + n_x^2}\right). \end{aligned} \tag{7}$$

Indexes 1, 2 are used for radiation generated in V_1 and V_2 correspondingly. Variable without the index means it is the same for radiation generated in V_1 and V_2. Using well-known expression for spectral-angular distribution

$$dW(\mathbf{n},\omega)/d\Omega d\omega = cr^2\left|E(\mathbf{r},\omega)\right|^2$$

we get:

$$\frac{dW(\mathbf{n},\omega)}{d\Omega d\hbar\omega} = \frac{1}{137}\left(\frac{\varepsilon - 1}{4\pi\beta_x}\right)^2\frac{e^{-2h\rho}}{\rho^2}\frac{\omega^4}{c^4}\left(q_1^{(j)} + q_2^{(j)} + q_3^{(j)}\right).$$

Here index $j = \mathrm{I}, \mathrm{II}$ corresponds to the cases I and II.

$$\begin{aligned} q_1^{(\mathrm{I})} = &\frac{\mathbf{A}^2 + \rho^2 - (\mathbf{A}\mathbf{n}_1)^2 - \rho^2 n_{1z}^2}{\rho^2 + \varepsilon\, n_{1z}^2\omega^2/c^2}\frac{\sin^2\left(N\varphi_1 d/2\right)}{\sin^2\left(\varphi_1 d/2\right)} \times \\ &\times\left\{\frac{4\sin^2\left(a\varphi_1/2\right)}{\varphi_1^2} + \frac{1 + e^{-2y_1 a} - 2e^{-y_1 a}\cos\left(ax_1\right)}{x_1^2 + y_1^2} - \right. \\ &\left. -\frac{4\sin\left(a\varphi_1/2\right)}{\varphi_1\left(x_1^2 + y_1^2\right)}\left(\cos\frac{\varphi_1 a}{2}\left[y_1 - D_1\right] + \sin\frac{\varphi_1 a}{2}\left[x_1 - R_1\right]\right)\right\}, \end{aligned}$$

$$\begin{aligned} q_2^{(\mathrm{I})} = &\frac{\mathbf{A}^2 + \rho^2 - (\mathbf{A}\mathbf{n}_2)^2 - \rho^2 n_{2z}^2}{\rho^2 + \varepsilon n_{2z}^2\,\omega^2/c^2}\frac{\sin^2\left(N\varphi_2 d/2\right)}{\sin^2\left(\varphi_2 d/2\right)} \times \\ &\times\left\{\frac{4\sin^2\left(\varphi_2 a/2\right)}{\varphi_2^2}e^{-2b\rho} + \frac{1 + e^{-2y_2 a} - 2e^{-y_2 a}\cos\left(ax_2\right)}{x_2^2 + y_2^2} - \right. \\ &-\frac{4\sin\left(a\varphi_2/2\right)}{\varphi_2\left(x_2^2 + y_2^2\right)}e^{-b\rho}\left[\cos\left(\sqrt{\varepsilon}k_{2z}b - \frac{\varphi_2 a}{2}\right)\left[y_2 - D_2\right] - \right. \\ &\left.\left. -\sin\left(\sqrt{\varepsilon}k_{2z}b - \frac{\varphi_2 a}{2}\right)\left[x_2 - R_2\right]\right]\right\}, \end{aligned}$$

$$\begin{aligned} q_3^{(\mathrm{I})} = &8\,\mathrm{Re}\left[\frac{\mathbf{n}_1\left(\mathbf{n}_1\mathbf{L}\right) - \mathbf{L}}{\rho - i\sqrt{\varepsilon}k_{1z}}F\frac{\mathbf{n}_2\left(\mathbf{n}_2\mathbf{L}^*\right) - \mathbf{L}^*}{\rho + i\sqrt{\varepsilon}k_{2z}}e^{i(\varphi_1 - \varphi_2)\left(a + (N-1)\frac{d}{2}\right)} \times \right. \\ &\times\left(\frac{\sin\left(\varphi_1 a/2\right)}{\varphi_1}e^{-\frac{ia\varphi_1}{2}} - \frac{1 - \exp\left[-ay_1 - iax_1\right]}{2\left(y_1 + ix_1\right)}\right) \times \\ &\left.\times\left(\frac{1 - \exp\left[-ay_2 + iax_2\right]}{2\left(y_2 - ix_2\right)} - e^{-b\left(\rho + i\sqrt{\varepsilon}k_{2z}\right)}e^{\frac{i\varphi_2 a}{2}}\frac{\sin\left(\varphi_2 a/2\right)}{\varphi_2}\right)\right], \end{aligned}$$

ISBN 978-3-95450-133-5

$$D_{(1,2)} = e^{-y_{(1,2)}a}\left[y_{(1,2)}\cos ax_{(1,2)} - x_{(1,2)}\sin ax_{(1,2)}\right],$$
$$R_{(1,2)} = e^{-y_{(1,2)}a}\left[x_{(1,2)}\cos ax_{(1,2)} + y_{(1,2)}\sin ax_{(1,2)}\right]$$
$$x_{(1,2)} = \varphi_{(1,2)} - \frac{n_{(1,2)z}}{n_{(1,2)x}}\sqrt{\varepsilon}k_{(1,2)z}, \qquad y_{(1,2)} = \frac{n_{(1,2)z}}{n_{(1,2)x}}\rho$$
$$F = \frac{\sin(N\varphi_1 d/2)}{\sin(\varphi_1 d/2)}\frac{\sin(N\varphi_2 d/2)}{\sin(\varphi_2 d/2)}$$

Now let us consider the **second case**. Here $n_z^2 \le 1-\varepsilon(\omega)$, i.e. the wave in the matter is evanescent. The total field of radiation has the form of Eq.(6), the spectral-angular distribution has the form of Eqs.(8), but here:

$$n_{1z} = -im_{1z},\ y_1 = \frac{-m_{1z}}{n_{1x}}\rho,\ x_1 = \varphi_1 + \sqrt{\varepsilon}m_{1z}\frac{\omega}{c}\frac{m_{1z}}{n_{1x}}$$
$$q_1^{(\mathrm{II})} = \frac{Q}{\left(\rho-\sqrt{\varepsilon}m_{1z}\,\omega/c\right)^2}\frac{\sin^2(N\varphi_1 d/2)}{\sin^2(\varphi_1 d/2)}\times$$
$$\times\left\{\frac{4\sin^2(a\varphi_1/2)}{\varphi_1^2} + \frac{4\sin^2((y_1+x_1)a/2)}{(y_1+x_1)^2} - \right.$$
$$\left. -\frac{8\sin(a\varphi_1/2)}{\varphi_1}\frac{\sin((y_1+x_1)a/2)}{y_1+x_1}\cos\left(\frac{(\varphi_1-x_1-y_1)a}{2}\right)\right\},$$

$q_2^{(\mathrm{II})} = q_2^{(\mathrm{I})}$ and x_2, y_2 are the same as in first situation.

$$q_3^{(\mathrm{II})} = 8\,\mathrm{Re}\frac{\mathbf{n}_1(\mathbf{n}_1\mathbf{L})-\mathbf{L}}{\rho-m_{1z}\sqrt{\varepsilon}\,\omega/c}\mathrm{F}\frac{\mathbf{n}_2(\mathbf{n}_2\mathbf{L}^*)-\mathbf{L}^*}{\rho+i\sqrt{\varepsilon}k_{2z}}e^{i(\varphi_1-\varphi_2)\left(a+\frac{d}{2}(N-1)\right)}$$
$$\times\left(\frac{\sin(\varphi_1 a/2)}{\varphi_1}e^{-\frac{i\varphi_1 a}{2}} - \frac{1-e^{-i(y_1+x_1)a}}{2i(y_1+x_1)}\right)\times$$
$$\times\left(\frac{1-\exp[-ay_2+iax_2]}{2(y_2-ix_2)} - e^{-b\left(\rho+i\sqrt{\varepsilon}k_{2z}\right)}e^{\frac{i\varphi_2 a}{2}}\frac{\sin(\varphi_2 a/2)}{\varphi_2}\right),$$
$$Q = \mathbf{A}^2+\rho^2-2\left[(\mathbf{A}\mathbf{n}_1)^2-m_{1z}^2\rho^2\right]+|\mathbf{n}_1|^2\left[(\mathbf{A}\mathbf{n}_1)-m_{1z}\rho\right]^2$$

ANALYSIS OF THE RESULTS

To analyse the results we put

$$n_x = \sin\theta\cos\phi,$$
$$n_y = \cos\theta, \qquad (9)$$
$$n_z = \sin\theta\sin\phi.$$

Moreover, we choose the value of angle $\theta = \arccos\left(\beta^{-1}\sin\alpha\right)$, because for it the exponent $e^{-2\rho h}$ in Eq. (8) has maximum, and the maximal radiation is distributed near the cone surface with the cone opening equal $\arccos\left(\beta^{-1}\sin\alpha\right)$ (in more detail see [7], [8]).

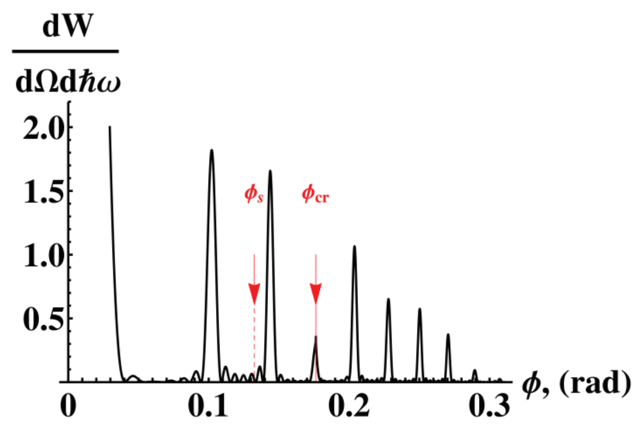

Figure 2: The total spectral-angular distribution of Smith-Purcell radiation. Here $\hbar\omega_p = 26.3\,eV$ (beryllium), $\gamma = 4\cdot 10^4$ (energy of FACET, SLAC), $N=7$, $\alpha = 30°$, $\theta = \arccos\left(\beta^{-1}\sin\alpha\right)$, $d = 1.5\,\mu m$, $a = d/4$, $b = 0.15\,\mu m$, $h = 60\,\mu m$, $\lambda = 6.75\,\mu m$, $\phi_{cr} = \arcsin\left(\sqrt{1-\varepsilon}/\sin\theta\right)$. For $\phi \le \phi_{cr}$ there are inhomogeneous evanescent waves in the medium, for $\phi \ge \phi_{cr}$ there are usual plane waves in the medium. For $\phi < \phi_s = \arctan\left[b/(d-a)\right]$ it is needed to take into account the radiation refracted on the forward edge of the strip and propagating through the next strips.

Figure 2 demonstrates the spectral-angular distribution of the radiation depending on the angle ϕ. It represents the set of peaks like usual Smith-Purcell radiation. The value of $dW(\mathbf{n},\omega)/d\Omega d\hbar\omega$ for $\phi = 0$ is maximal and equals ≈ 19.8 for parameters taken. Obtaining Eq. (8), we suppose rather big grating period:

$$(d-a)n_{2z}/n_{2x} \ge b. \qquad (10)$$

We do so in order not to consider the radiation generated in one strip and going through the next strips, which would require much more complicated calculation.

Solving the inequality (10) relative to ϕ with help of Eq. (9), it is easy to get the restriction

$$\phi > \phi_s = \arctan\left[b/(d-a)\right]. \qquad (11)$$

The minimal value ϕ_s is shown in Fig. 2 as red dashed line with arrow. To consider the area of $\phi < \phi_s$ one should take into account the radiation refracted on the forward edge of the strip and propagating through the next strips. As we said above, there is some critical value $n_z^{cr} = \sqrt{1-\varepsilon(\omega)}$ or, using the third of Eqs. (9), there is

$$\phi_{cr} = \arcsin\left(\sqrt{1-\varepsilon}/\sin\theta\right). \qquad (12)$$

For $\phi \le \phi_{cr}$ there are inhomogeneous plane (evanescent) waves in the medium, for $\phi \ge \phi_{cr}$ there are usual plane waves in the medium. The value ϕ_{cr} is shown in Fig. 2 as

ISBN 978-3-95450-133-5

thin red line with arrow. Figure 2 is plotted up to the value

$$\phi_{max} = \min\left\{\arccos\left(\frac{\sqrt{1-\varepsilon(\omega)}}{\sin\theta}\right);\arctan\left(\frac{b}{a}\right)\right\}. \quad (13)$$

The first quantity in braces arises from the inequality $n_x^2 \geq \varepsilon(\omega)-1$, the second one arises from the condition

$$b \geq a\, n_{2z}/n_{2x}, \quad (14)$$

which is of common sense for thick enough strips; for thin strips the independent calculations are required.

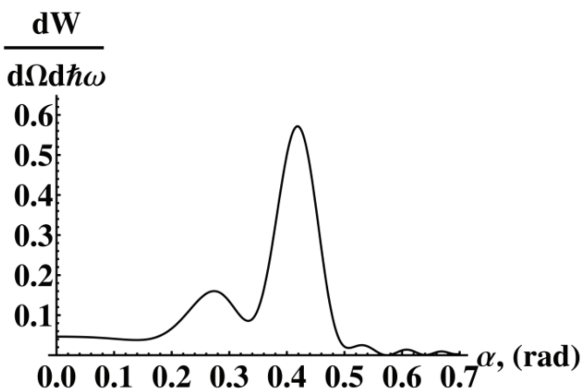

Figure 3: The total spectral-angular distribution of the Smith-Purcell radiation depending on α. Here $\phi = 0.2\,rad$ and other parameters the same as in Fig. 2.

Figure 3 demonstrates the spectral-angular distribution in dependence on the angle between trajectory of the particle and the grating rulings. We would like to notice that with the growing of α the angle $\theta = \arccos\left(\beta^{-1}\sin\alpha\right)$ changes. This graph shows the radiation in the plane perpendicular to the *xz*-plane and at constant angle to the grating plain. One can see that for fixed value of viewing angle ϕ and for $\alpha = 0$ the radiation is not maximal. It is possible to observe more intensive radiation turning the grating relative to *z*-axis. The different maxima in Fig. 3 correspond to the peaks of Smith-Purcell radiation (different diffraction orders).

CONCLUSION

We developed theory for the radiation from the single particle moving parallel to the grating surface at arbitrary angle to the rulings direction. Refraction of radiation on both target edges proves to influence significantly on Smith-Purcell radiation spectrum in UV and soft X-ray ranges of frequency.

It was shown that for fixed value of observation angle and for particle moving perpendicular to the ruling direction the radiation is not maximal: it is possible to observe more intensive radiation turning the grating relative to *z*-axis.

REFERENCES

[1] A. P. Potylitsyn *et al.*, Diffraction Radiation from Relativistic Particles, Berlin: Springer-Verlag, 2011.

[2] D. Yu. Sergeeva *et al.*, “UV and X-ray diffraction and transition radiation from charged particles bunches,” *Nucl. Instruments and Methods B,* vol. 309, p. 189, 2013.

[3] A. A. Tishchenko *et al.,* “Diffraction radiation from an ultrarelativistic charge in the plasma frequency limit,” *Phys. Rev. E,* vol. 70, p. 066501, 2004.

[4] H. L. Andrews *et al.,* “Reconstruction of the time profile of 20.35 GeV, subpicosecond long electron bunches by means of coherent Smith-Purcell radiation,” *Phys. Rev. ST AB,* vol. 17, p. 052802, 2014.

[5] W. Knulst *et al.,* “High brightness, narrowband, and compact soft x-ray Cherenkov sources in the water window,” *Appl. Phys. Lett.,* vol. 83, p. 4050, 2003.

[6] A. A. Tishchenko *et al.,* “X-ray diffraction radiation in conditions of Cherenkov effect,” *Phys. Lett. A,* vol. 359, p. 509, 2006.

[7] A. A. Tishchenko et al., “Backward Smith-Purcell Radiation,” in *Proc. of RREPS 2013*, Erevan, Armenia, 2013.

[8] O. Haeberle et al., “Smith-Purcell radiation from electrons moving parallel to a grating,” *Phys. Rev. E,* vol. 55, p. 4675, 1997.

ISBN 978-3-95450-133-5